Decomposed Modeling of Controllable and Uncontrollable Components in Power Systems with High Penetration of Renewable Energies

Hai Li, Ning Zhang, Yue Fan, Ling Dong, and Pengcheng Cai

***Abstract*—The high penetration of variable renewable energies requires the flexibility from both the generation and demand sides. This raises the necessity of modeling stochastic and flexible energy resources in power system operation. However, some distributed energy resources have both stochasticity and flexibility, e.g., prosumers with distributed photovoltaics and energy storage, and plug-in electric vehicles with stochastic charging behavior and demand response capability. Such partly controllable participants pose challenges to modeling the aggregate behavior of large numbers of entities in power system operation. This paper proposes a new perspective on the aggregate modeling of such energy resources in power system operation. Specifically, a unified controllability-uncontrollability-decomposed model for various energy resources is established by modeling the controllable and uncontrollable parts of energy resources separately. Such decomposition enables the straightforward aggregate modeling of massive energy resources with different controllabilities by integrating their controllable components with linking constraints and uncontrollable components with dependent discrete convolution. Furthermore, a two-stage stochastic unit commitment model based on the proposed model for power system operation is established. The proposed model is tested using a three-bus system and real Qinghai provincial power grid of China. The result shows that this model is able to characterize at high accuracy the aggregate behavior of massive energy resources with different levels of controllability so that their flexibility can be fully explored.**

***Index Terms*—Aggregation, dependent discrete convolution, flexibility, stochastic unit commitment, virtual power plant.**

NOMENCLATURE

A. Indices

c	Index of generator clusters (from 1 to N_C)
g	Index of generators (from 1 to N_G)
l	Index of transmission lines (from 1 to N_L)
n	Index of nodes (from 1 to N_N)
s	Index of scenarios (from 1 to N_S)
t	Index of time periods (from 1 to N_T)

B. Decision Variables

$L_{n,t}^{Cur}$	Unserved load on node n during time period t
$P_{g,t}$	Output of generator g during time period t
$P_{g,t}^{c}/P_{g,t}^{u}$	Controllable/uncontrollable component of $P_{g,t}$
$R_{c,t}^{Ru}/R_{c,t}^{Rd}$	Scheduled up/down reserve of cluster c during time period t
$SU_{c,t}/SD_{c,t}$	Startup/shutdown capacity of cluster c during time period t
$\widetilde{(\cdot)}$	Real-time variables in a certain scenario s

C. Parameters

θ^{VoLL}	Coefficient of unserved load penalty
π_s^{RT}	Probability of scenario s
$\underline{C}_{g,t}/\overline{C}_{g,t}$	Lower/upper power limit of generator g during time period t
C_c^{SU}	Coefficient of startup cost of cluster c
C_c	Coefficient of energy cost of cluster c
C_c^{Ru}/C_c^{Rd}	Coefficients of up/down reserve capacity costs of cluster c
$\underline{DC}_{g,t}/\overline{DC}_{g,t}$	Lower/upper ramping limit of generator g during time period t
$\overline{F}_l^L$	Transmission capacity limit of line l
G_n^l	Generation shift distribution factor of line l and node n
$L_{n,t}^{fore}$	Forecast load of node n during time period t
N_C	Total number of generator clusters
N_G	Total number of generators
N_L	Total number of transmission lines
N_N	Total number of nodes

Manuscript received: September 11, 2020; revised: March 10, 2021; accepted: July 26, 2021. Date of CrossCheck: July 26, 2021. Date of online publication: September 15, 2021.

This work was supported by the Science and Technology Project of the State Grid Corporation of China (No. SGJSJY00GHJS2100183).

H. Li and N. Zhang (corresponding author) are with the State Key Laboratory of Power Systems, Department of Electrical Engineering, Tsinghua University, Beijing 100084, China (e-mail: lihai17@mails.tsinghua.edu.cn; ningzhang@tsinghua.edu.cn).

Y. Fan and L. Dong are with State Grid Qinghai Electric Power Co., Ltd., Xining, China (e-mail: 1016061587@qq.com; 154951400@qq.com).

P. Cai is with State Grid Xinjiang Electric Power Co., Ltd., Urumqi, China (e-mail: 695956806@qq.com).

DOI: 10.35833/MPCE.2020.000674

N_S	Total number of scenarios
N_T	Total number of time periods
$o_{c,t}$	On-line rate of cluster c during time period t, ranging from 0 to 1
$R^{Ru,sys}/R^{Rd,sys}$	Up/down reserve requirement of whole system
$\underline{SC}_{g,t}/\overline{SC}_{g,t}$	Lower/upper energy limit of generator g during time period t

D. Sets

Ω_c	Set of generators belonging to cluster c
Ω_n	Set of generator clusters connected to node n

I. Introduction

POWER system operation has been significantly changed by new participants in the past few decades. Traditionally, the generation side has been fully controllable and the demand side fully uncontrollable in terms of active power. The goal of the power system is to use the fully controllable generators to satisfy the uncontrollable active power demand. With the integration of variable renewable energy, uncertainty is introduced into the generation side. Hence, the generation side becomes partly uncontrollable. In recent years, the emergence of demand response and demand-side energy storage system (ESS) has added flexibility to uncontrollable loads. The loads have therefore become partly controllable. A transition to using partly uncontrollable resources to balance the partly controllable load demand is required for power system dispatch.

The modeling of partly controllable energy resources poses challenges in power system operation optimization since a clear distinction is drawn between controllable and uncontrollable energy resources in the existing power systems. Traditionally, variable renewable energy is considered as a fully uncontrollable energy resource, while thermal units are regarded as a fully controllable energy resource. However, distributed energy resources that have both controllable and uncontrollable characteristics, e.g., prosumers with uncontrollable distributed photovoltaics (PV), ESS, and plug-in electric vehicles (PEVs) with stochastic charging behavior and demand response capability, are being continuously integrated into power systems. Such partly controllable participants need to be modeled and considered in power system dispatch as the resources to be optimized. Furthermore, an aggregate model is required for such participants since the amount is very large and they cannot be modeled individually. How to model and aggregate controllable and uncontrollable energy resources remains an open question in power system operation.

Stochastic models are the basis for capturing the uncontrollable characteristics in power system operation. The probability distribution is typically used to characterize the uncertainty. Scenarios and scenario trees are proposed by enumerating the possible future outcomes according to a probability distribution. Based on the description of uncertainty, two-stage and multiple-stage stochastic unit commitment (SUC) models [1] are proposed to ensure that the power system can handle such uncertainty. Reference [2] proposes a data-driven method for characterizing the uncertainty of wind power instead of assuming the true distribution of wind power output. Reference [3] proposes a scenario map model to integrate a large number of scenarios into a compact model while preserving the uncertainty and variability features of wind power. Instead of fully accommodating the uncertainty of variable renewable energy, several studies also discuss the possibility of allowing wind power to provide reserves to the power systems [4]-[6].

Recent studies also focus on modeling flexibility on the demand side [7], i.e., modeling demand response (DR) and demand-side ESS. For DR, both price-based DR and incentive-based DR have been introduced to broaden the flexibility of the demand side. Reference [8] models the residential load as a completely controllable resource to study the operation model of a residential hybrid energy system based on the price response. Reference [9] proposes a reward-based DR algorithm for residential customers to reduce network peaks, in which the uncertainty of the residential customer's behavior is not taken into account. Reference [10] models the parking lots as a flexible resource to study the optimal strategy of the parking lots considering the uncertainty of car arrival.

Attention has been paid to modeling the flexibility for demand-side ESS. Reference [11] studies the optimal operation of a neighborhood of smart household that comprises PEV, distributed energy storage (DES) and distributed generation (DG). Reference [12] proposes a hierarchical energy management system to aggregate multiple battery energy storage systems (BESSs) to participate in the energy and frequency regulation market. Reference [13] proposes a new type of DES named cloud energy storage capable of providing energy storage services at a substantially lower cost. However, the above studies model the demand-side ESS as a fully controllable energy resource, ignoring the inherent uncontrollable characteristics of ESS due to user interference.

Additionally, there are studies focusing on the aggregation of energy resources with different controllabilities, e.g., a virtual power plant (VPP) [14], which is defined as a combination of different distributed energy resources that operate as a single entity. Reference [15] addresses the optimal bidding strategy problem of a VPP considering the uncertainty of wind farms and elasticity of demand. Reference [16] proposes a model for the day-ahead self-scheduling problem of a VPP trading in both the energy and reserve electricity markets, considering the uncertainty of wind farms and the flexibility of ESS. In these studies, the energy resources in the VPP need to be modeled individually.

The litterature review shows that the current uncertainty model for power system operation cannot fully address the issue of modeling and aggregating controllable and uncontrollable energy resources. Since current models establish either a fully controllable or a fully uncontrollable model for energy resources with different controllabilities, it is difficult to aggregate energy resources with different controllabilities,

e.g., a generation company with multiple variable renewable energy stations bundled with flexible generators and ESS and a load aggregator with massive distributed PV and demand response units. If such energy resources participate in the power system operation as one entity, they cannot be modeled as either a fully controllable or a fully uncontrollable energy resource.

In this paper, we propose a new perspective on the controllability of these energy resources. Each energy resource participating in power system operation is considered to have both controllable and uncontrollable characteristics, in which the controllable and uncontrollable parts are modeled separately. Such modeling facilitates a rigorous aggregation of energy resources with different controllabilities. The contributions of this paper are threefold: ① a controllability-uncontrollability-decomposed (CUD) model that unifies the operation models of different types of generators, controllable loads, and ESS; ② the principle of aggregating CUD models of energy resources with different controllabilities; and ③ a CUD-model-based unit commitment model for power system operation.

The remainder of the paper is organized as follows. Section II states the basic framework of the CUD model. Section III describes the CUD model for various energy resources. Section IV proposes the aggregate model for massive energy resources based on the CUD model. Section V establishes a two-stage unit commitment model based on the aggregate CUD model. Section VI analyzes the aggregate model using an illustrative three-bus system. Section VII provides the results from a real case study using Qinghai provincial power grid of China. Finally, conclusions are drawn in Section VIII.

II. Problem Statement and Framework of CUD Model

The purpose of building the CUD model is to aggregate a large number of different types of generators, controllable loads, and ESS as a single generator that participates in power system operation while keeping their original operating characteristics. Since it is difficult to aggregate energy resources with different controllabilities, the precondition of aggregation is that the model of each energy resource should be of the same mathematical form. To model the energy resources with different controllabilities using the same mathematical form, we consider all of the energy resources, e.g., generators, controllable loads, and ESS, to have controllable and uncontrollable characteristics at the same time. For example, wind power can be scheduled to operate at a derated output to reduce the uncertainty caused by wind power generation and provide additional system reserves. Hence, the stochastic generators are also characterized by some controllabilities. Additionally, the output of thermal and hydropower units may be uncertain due to a lack of fuel supply, water inflow, or unit failure. Therefore, flexible generators may also be characterized by uncontrollability to some extent. Furthermore, some generators, such as those concentrating solar power (CSP) generators, are inherently characterized by the uncontrollability of the power source and controllability of the output.

As has been discussed above, it is inappropriate to consider only the stochasticity or flexibility of each energy resource. Inspired by the superposition theorem in circuit theory, we decompose the output of each energy resource into two components: the controllable component and the uncontrollable component. The controllable component is defined as the part of electricity production or consumption that can be modified in response to an external signal (price signal or activation) to provide a service within the energy system. It can be modeled by operating constraints. The uncontrollable component is defined as the part of electricity production or consumption that cannot be known in advance in power system operation. It is modeled as a stochastic variable following certain probability distribution functions (PDFs). By doing so, the aggregation of energy resources with different controllabilities can be implemented by aggregating the controllable components and uncontrollable components. Figure 1 illustrates the framework of the proposed methodology.

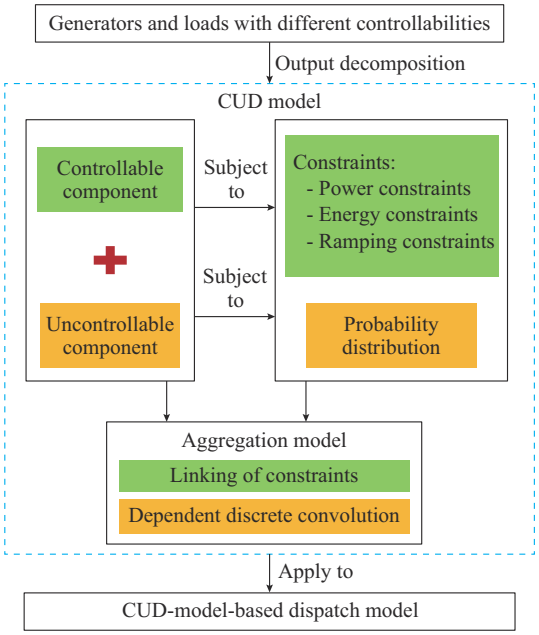

Fig. 1. Framework of proposed methodology.

It should be noted that in this paper, the concepts of controllability and uncontrollability are different from those of flexibility and stochasticity, respectively. The former two terms denote the physical capacities that can and cannot be controlled, while the latter two terms denote the characteristics of a generator or a load. For example, wind power and PV are regarded as stochastic generators, but they are regarded as having both controllable and uncontrollable components.

The proposed framework transforms the problem into three subproblems. First, the determination of controllable and uncontrollable components of all kinds of energy resources in the power system will be addressed in Section III. Second, the aggregation of controllable and uncontrollable components of a large unit consisting of multiple energy resources will be addressed in Section IV. Third, dispatching these aggregate energy resources will be addressed in Section V.

III. Unified CUD Model for Different Types of Generators and Loads

A. Unified CUD Model

The purpose of the CUD model is to build a unified model for all types of generators and loads to simultaneously capture their controllable and uncontrollable components. Mathematically, a generator/load is the sum of a controllable component and an uncontrollable component, as shown in (1).

$$P_{g,t}=P^{c}_{g,t}+P^{u}_{g,t} \tag{1}$$

where the output of each energy resource $P_{g,t}$ is decomposed into a controllable component $P^{c}_{g,t}$ and an uncontrollable component $P^{u}_{g,t}$.

Such decomposition facilitates the decoupled modeling of each component. The controllable component is modeled by a series of constraints, i. e., power constraints, energy constraints, and ramping constraints. A unified model for the controllable component $P^{c}_{g,t}$ can be expressed as:

$$\begin{cases} \underline{C}_{g,t}\le P^{c}_{g,t}\le \overline{C}_{g,t} \\ \underline{SC}_{g,t}\le \sum_{t'=1}^{t} P^{c}_{g,t'}\le \overline{SC}_{g,t} \\ \underline{DC}_{g,t}\le P^{c}_{g,t}-P^{c}_{g,t-1}\le \overline{DC}_{g,t} \end{cases} \tag{2}$$

The uncontrollable component $P^{u}_{g,t}$ is modeled as a stochastic process $\{P^{u}(t), t\in T\}$. For a single time interval, $P^{u}(t_n)$ is a random variable. It follows a certain PDF:

$$P^{u}(t_n)\sim f\left(P^{u}(t_n)\right) \tag{3}$$

The unified CUD model applies to various energy resources, e. g., wind power, PV, thermal units, gas turbines, ESS, hydropower, and CSP. Each resource type has its specific CUD model and is described in the following subsections.

B. Wind Power and PV

Natural-resource-constrained units such as wind farms and PV stations are considered to be flexible in that they can be scheduled to operate at a derated output to provide down and up reserves; hence, the capacity between zero and the forecasted output can be regarded as the controllable component. However, such flexibility is uncertain due to the incorrect forecasting; therefore, the forecasting error is considered as the uncontrollable component. The energy constraint of wind farms and PV stations is unbounded since it is determined by natural resources of wind and solar radiation, respectively. The ramp constraint is also unbounded since the adjustment of wind generators and PV inverters is very rapid. Thus, the CUD model of wind and PV power units can be expressed as:

$$\begin{cases} P_{g,t}=P^{c}_{g,t}+P^{u}_{g,t} \\ 0\le P^{c}_{g,t}\le P^{fore}_{g,t} \\ \sum_{t'=1}^{t} P^{c}_{g,t'} \quad \text{constraint not required} \\ P^{c}_{g,t}-P^{c}_{g,t-1} \quad \text{constraint not required} \\ P^{u}_{g,t}\sim f\left(Err^{u}_{g,t}\right) \end{cases} \tag{4}$$

where $P^{fore}_{g,t}$ is the point forecasting output; and $Err^{u}_{g,t}$ is the forecasting error.

C. Thermal Units and Gas Turbines

Coal-fueled and oil-fueled thermal units and gas turbines are regarded as flexible generators and can be scheduled to operate between their technical minimum power and the rated power. Their outputs are constrained by the maximum ramping down and up rates determined by the thermal dynamics of the steam turbine. This is considered to be the controllability of this type of unit, while the uncontrollability arises from the forced outages. The fuel constraints drive the units' energy limits. Thus, the CUD model of thermal units and gas turbines is given by:

$$\begin{cases} P_{g,t}=P^{c}_{g,t}+P^{u}_{g,t} \\ x_{g,t}\underline{P}_{g}\le P^{c}_{g,t}\le x_{g,t}\overline{P}_{g} \\ \sum_{t'=1}^{t} P^{c}_{g,t'} \quad \text{constraint not required} \\ x_{g,t}\overline{P}^{ramp,dn}_{g}+\left(1-x_{g,t}\right)\overline{P}^{ramp,sd}_{g}\le P^{c}_{g,t}-P^{c}_{g,t-1}\le \\ \qquad x_{g,t-1}\overline{P}^{ramp,up}_{g}+\left(1-x_{g,t-1}\right)\overline{P}^{ramp,su}_{g} \\ f\left(P^{u}_{g,t}\right)=\begin{cases} q_g & P^{u}_{g,t}=0 \\ 1-q_g & P^{u}_{g,t}=-P^{c}_{g,t} \end{cases} \end{cases} \tag{5}$$

where $x_{g,t}$ is a binary variable denoting the on/off status of the unit ($x_{g,t}=1$ represents the generator is on); $\overline{P}^{ramp,dn}_{g}$ and $\overline{P}^{ramp,up}_{g}$ are the maximum ramping down and up rates during the operation, respectively; $\overline{P}^{ramp,sd}_{g}$ and $\overline{P}^{ramp,su}_{g}$ are the shutdown and startup ramping rates, respectively; and q_g is the probability that the unit is operating in the normal state.

D. ESSs

An ESS can be scheduled to operate between its maximum discharging and maximum charging power levels. The stored energy must be within the minimum and maximum energy capacities, which form the energy constraint. The ramp constraint is unbounded since the adjustment of the rectifier and inverter is very fast. Thus, the CUD model of an ESS is given by:

$$\begin{cases} P_{g,t}=P^{c}_{g,t}+P^{u}_{g,t} \\ P^{c}_{g,t}=P^{c,c}_{g,t}-P^{c,d}_{g,t} \\ 0\le P^{c,c}_{g,t}\le \overline{P}_{g} \\ 0\le P^{c,d}_{g,t}\le -\underline{P}_{g} \\ \underline{E}_{g}\le \sum_{t'=1}^{t}\left(\eta^{c}_{g}P^{c,c}_{g,t'}-\dfrac{P^{c,d}_{g,t'}}{\eta^{d}_{g}}\right)\Delta t+E_{g,0}\le \overline{E}_{g} \\ 0\le \sum_{t'=1}^{t}\left(\eta^{c}_{g}P^{c,c}_{g,t'}-\dfrac{P^{c,d}_{g,t'}}{\eta^{d}_{g}}\right)\Delta t\le 0 \quad t=T_{end} \\ P^{c}_{g,t}-P^{c}_{g,t-1} \quad \text{constraint not required} \\ f\left(P^{u}_{g,t}\right)=\begin{cases} q & P^{u}_{g,t}=0 \\ 1-q & P^{u}_{g,t}=-P^{c}_{g,t} \end{cases} \end{cases} \tag{6}$$

where Δt is the time interval; T_{end} is the time period of the end of an energy balancing cycle, e.g., a whole day; $\underline{E}_g$, $\overline{E}_g$, and $E_{g,0}$ are the minimum energy capacity, the maximum energy capacity, and the initial stored energy of the ESS, respectively; the non-negative variables $P_{g,t}^{c,c}$ and $P_{g,t}^{c,d}$ are the charging and discharging power of the ESS, respectively; and η_g^c and η_g^d are the charging and discharging efficiency of the ESS, respectively.

E. Hydropower and CSP

Both hydropower and CSP have uncertain primary energy inputs (water inflow and solar radiation, respectively), similar to wind power and PV. At the same time, they are flexible in their outputs since they both have the ability to store the energy. Therefore, their model is a combination of a stochastic generator and an ESS. The uncontrollable component can be regarded as the water inflow or solar radiation (converted to the equivalent power output), while the controllable component can be regarded as the difference between the scheduled output and the input. Hydropower and CSP can be scheduled to operate between the minimum and maximum outputs. The stored energy must be within the minimum and maximum energy capacities, which form the energy constraint. Their outputs are constrained within the maximum ramping down and up rates determined by the dynamics of the hydro turbine and the power block, respectively. Thus, their model is shown in (7).

$$\begin{cases} P_{g,t}=P_{g,t}^{c}+P_{g,t}^{u} \\ \underline{P}_g-P_{g,t}^{u}\le P_{g,t}^{c}\le \overline{P}_g-P_{g,t}^{u} \\ \underline{E}_g\le-\sum_{t'=1}^{t}P_{g,t'}^{c}\Delta t+E_{g,0}\le \overline{E}_g \quad t=1,2,...,T_{end}-1 \\ E_{g,end}\le-\sum_{t'=1}^{t}P_{g,t'}^{c}\Delta t+E_{g,0}\le E_{g,end} \quad t=T_{end} \\ \overline{P}_g^{ramp,dn}-P_{g,t}^{u}+P_{g,t-1}^{u}\le P_{g,t}^{c}-P_{g,t-1}^{c}\le \overline{P}_g^{ramp,up}-P_{g,t}^{u}+P_{g,t-1}^{u} \\ P_{g,t}^{u}\sim f\left(P_{g,t}^{fore}\right) \end{cases} \tag{7}$$

For hydropower, $P_{g,t}^{fore}$ is the forecasted probability of water inflow (converted to the equivalent power output); $\underline{P}_g$ and $\overline{P}_g$ are the lower and upper output limits of the hydro turbine, respectively; $\underline{E}_g$ and $\overline{E}_g$ are the minimum and maximum capacities of the reservoir (converted to the equivalent energy capacity), respectively; $E_{g,0}$ is the initial amount of stored water of the reservoir; and $E_{g,end}$ is the scheduled amount of final stored water of the reservoir after a certain period, e.g., one day. Note that if the hydropower does not have a reservoir, it does not have the capability to store energy. In this case, the model would be similar to the wind power and PV as shown in (5).

For CSP, $P_{g,t}^{fore}$ is the forecasted probability of solar radiation (converted to the equivalent power output); $\underline{P}_g$ and $\overline{P}_g$ are the lower and upper power limits of the power block, respectively; $\underline{E}_g$ and $\overline{E}_g$ are the minimum and maximum capacities of thermal energy storage (converted to the equivalent energy capacity), respectively; $E_{g,0}$ is the initially stored heat; and $E_{g,end}$ is the scheduled final stored heat of the reservoir after a certain period.

Note that the above model ignores the nonlinearity of the energy conversion process. Such nonlinearity can be modeled through piecewise linearization, which essentially splits one generator into multiple ones. Such a modeling technique has already been considered in the current literature and is not discussed in this paper.

F. Controllable Load

Controllable loads refer to the loads that can be curtailed as long as the compensation fees are paid for the unserved loads. Hence, they are controllable from zero to the forecasted load. Besides, due to the incorrect load forecasting, the controllable loads also have uncontrollability which can be described by the forecasting error. Thus, the CUD model of controllable loads can be expressed as:

$$\begin{cases} L_{g,t}=L_{g,t}^{c}+L_{g,t}^{u} \\ 0\le L_{g,t}^{c}\le L_{g,t}^{fore} \\ \sum_{t'=1}^{t}L_{g,t'}^{c} \quad \text{constraint not required} \\ L_{g,t}^{c}-L_{g,t-1}^{c} \quad \text{constraint not required} \\ L_{g,t}^{u}\sim f\left(Err_{g,t}^{u}\right) \end{cases} \tag{8}$$

where $L_{g,t}^{fore}$ is the point forecasting value of the load.

IV. Aggregation Methodology for CUD Model

According to the "superposition theorem", the aggregation of CUD models of various kinds of generators and loads is performed by aggregating their controllable components and uncontrollable components separately.

A. Aggregation of Controllable Components

Controllable components are usually described by three kinds of constraints: power, energy, and ramping constraints. When multiple energy resources are considered as a whole, their overall controllability is the sum of all individual controllability values. Mathematically, the lower and upper constraints of controllable components $P_{c,t}^{c}$ can be obtained by summing the lower and upper bounds of all corresponding constraints, respectively, as shown in (9).

$$\begin{cases} \underline{C}_{c,t}=\sum_{g\in\Omega_c}\underline{C}_{g,t} \\ \overline{C}_{c,t}=\sum_{g\in\Omega_c}\overline{C}_{g,t} \\ \underline{SC}_{c,t}=\sum_{g\in\Omega_c}\underline{SC}_{g,t} \\ \overline{SC}_{c,t}=\sum_{g\in\Omega_c}\overline{SC}_{g,t} \\ \underline{DC}_{c,t}=\sum_{g\in\Omega_c}\underline{DC}_{g,t} \\ \overline{DC}_{c,t}=\sum_{g\in\Omega_c}\overline{DC}_{g,t} \end{cases} \tag{9}$$

Thus, the constraints of controllable component can be expressed as:

$$\begin{cases} o_{c,t}K_c^C\underline{C}_{c,t} \le P_{c,t}^c \le o_{c,t}K_c^C\overline{C}_{c,t} \\ o_{c,t}K_c^S\underline{SC}_{c,t} \le \sum_{t'=1}^{t} P_{c,t'}^c \le o_{c,t}K_c^S\overline{SC}_{c,t} \\ o_{c,t}K_c^D\underline{DC}_{c,t} \le P_{c,t}^c - P_{c,t-1}^c \le o_{c,t}K_c^D\overline{DC}_{c,t} \end{cases} \tag{10}$$

For thermal unit and gas turbine clusters which have start-up costs, $o_{c,t}$ reflects the on-off status of the units, hence $o_{c,t}$ is related with the total startup costs of the cluster. For other units that do not have startup costs, $o_{c,t}$ always equals to 1, which means all the units are on-line [17].

The parameters K_c^C, K_c^S, and K_c^D are the modifed power coefficient, energy coefficient and ramping coefficient of cluster c, respectively, which are used to discount the capability of each cluster so as to avoid the overestimation of flexibility in the aggregate model. For example, if none of the controllable components of all the units in a cluster reaches the upper limit or lower limit, the cluster will have full ramping capability so that $K_c^D = 1$. Otherwise, K_c^D would be smaller than 1, whose value can be obtained through a data-driven analysis using historical data. Figure 2 illustrates how to determine K_c^D. The x-axis represents the difference between the controllable component $P_{c,t}^c$ and its upper limit. The y-axis represents the ramping capability. Each red circle represents a historical operation state. If we assume $K_c^D = 1$, the feasible region would be the trapezoid below the green line. All the points are inside the area, which means using the green line will lead to an overestimation of ramping capability. If we assume $K_c^D = \overline{D}_{c,t}/\overline{C}_{c,t}$, the feasible region would be the triangle below the yellow line, which will lead to an underestimation of ramping capability. To obtain a more accurate model, regression methods could be used to determine K_c^D, shown as the blue dashed line.

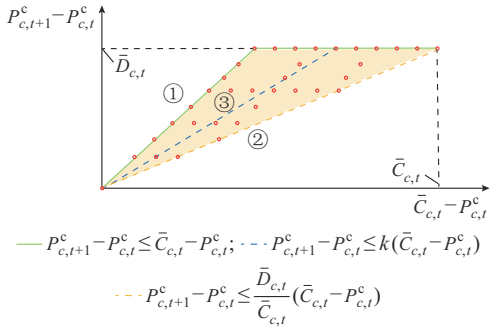

Fig. 2. Estimation for modified ramping coefficient K_c^D.

The rule of aggregation of controllable components is that an energy resource with a certain kind of unbounded constraint cannot be merged with others that have bounded constraints of the same kind, e. g., an energy resource with an unbounded ramping constraint cannot be aggregated with other energy resources that have bounded ramping constraints. Otherwise, their aggregate energy will be partially constrained. Only the resources with the same set of bounded constraints can be aggregated into the same energy resource; otherwise, they need to be modeled separately.

B. Aggregation of Uncontrollable Components

Uncontrollable components are described by PDFs, so their aggregation can be achieved by convolutions. However, uncontrollable components may have mutual dependencies [18], e. g., the forecasting errors of multiple adjacent wind farms or PV stations can be highly dependent. For the dependent uncontrollable components, dependent discrete convolution (DDC), which is an extension of the probabilistic convolution proposed in [19], is used. With known marginal PDFs of uncontrollable components $F_1(P_{1,t}^u)$, $F_2(P_{2,t}^u)$, and the copula function $c(F_1(P_{1,t}^u), F_2(P_{2,t}^u))$ among them, the PDF of the aggregation $P_{com,t}^u$ can be calculated as:

$$\begin{cases} \mathbb{P}\left(P_{com,t}^u(j\Delta p)\right) = \sum_{m+n=j} s_c(m\Delta p, n\Delta p) \cdot \\ \qquad \mathbb{P}_1\left(P_{1,t}^u(m\Delta p)\right) \cdot \mathbb{P}_2\left(P_{2,t}^u(n\Delta p)\right) \\ s_c(m\Delta p, n\Delta p) = c\left(\sum_{i=\underline{\tilde{P}}_{1,t}^u/\Delta p}^{m} \mathbb{P}_1\left(P_{1,t}^u(i\Delta p)\right), \sum_{i=\underline{\tilde{P}}_{2,t}^u/\Delta p}^{n} \mathbb{P}_2\left(P_{2,t}^u(i\Delta p)\right)\right) \end{cases} \tag{11}$$

where Δp is the discretization step; and $\underline{\tilde{P}}_{1,t}^u$ and $\underline{\tilde{P}}_{1,t}^u$ are the discretized lower bounds of $P_{1,t}^u$ and $P_{2,t}^u$, respectively.

Furthermore, the DDC of two uncontrollable components can be extended to N components. The computational complexity of a high-dimensional DDC can be reduced to linear complexity by utilizing the independence of variables [20].

V. CUD-Model-Based SUC Model

Based on the CUD model, an SUC model can be built to optimize the generation schedule while considering the controllability and uncontrollability for all energy resources. In this paper, a scenario-based two-stage CUD-model-based SUC model is established. It should be noted that other kinds of SUC models such as the robust model, chance-constrained model, and risk-based model can also be built based on the CUD model. For robust models, they try to find the optimal solution for the worst scenario through PDF. Mathematically, the uncertainty set is obtained from the PDF of the stochastic variable. For the chance-constrained model, the PDF can be directly used in the chance constraints. For the risk-based model, the PDF can be used to formulate the associated risks. To sum up, the aggregate model is irrespective of the optimization model since the proposed aggregate model aims at how to yield the aggregate PDF of uncontrollable components and the aggregation of controllable components.

A. Model Framework

The proposed model simultaneously optimizes the energy and reserve scheduling decisions considering the uncertainty. The uncertainty input at the same bus is modeled by PDFs and then aggregated using DDC. The uncertainty input at different buses is modeled by multiple scenarios. The proposed model has a two-stage structure. The first stage optimizes the day-ahead scheduling based on point forecasting results,

while the second stage eliminates the power imbalance for all possible realizations in real time. The SUC model is optimized to minimize the overall expected operation cost.

The variables associated with each stage are explained as follows. For the first stage, the variables include: ① scheduled power output of each unit; ② scheduled down/up spinning reserve of each unit; and ③ power flow on each branch. These variables are referred to as here-and-now decisions and do not depend on any particular scenario realization. For the second stage, the variables pertain to each particular scenario for real-time re-dispatch, including: ① deployment of down/up spinning reserve of each unit; ② load shedding at each bus; and ③ actual power flow on each branch. These variables are referred to as wait-and-see decisions. The proposed model differs from the traditional SUC model in that all of distributed energy resources can be modeled together using the proposed CUD model. Using such a model, the controllability and uncontrollability of all types of energy resources are well captured so that the utilization of flexibility of all types of resources can be well optimized to tackle the uncertainty of such resources.

B. Model Formulation

1) Objective Function

The objective function C^{sys} consists of two parts: the day-ahead cost $C^{DA,sys}$ and the real-time cost $C_s^{RT,sys}$, which are shown in (12)-(14). The day-ahead cost includes the startup cost, fuel cost and up and down reserve scheduling cost. The real-time cost includes the reserve deployment cost and the penalty cost of load shedding.

$$\min C^{sys} = C^{DA,sys} + \sum_{s=1}^{N_S} \pi_s^{RT} C_s^{RT,sys} \tag{12}$$

$$C^{DA,sys} = \sum_{t=1}^{N_T}\sum_{c=1}^{N_C}\left(C_c^{\mathrm{SU}} SU_{c,t} + C_c P_{c,t}^{\mathrm{c}} + C_{\mathrm{c}}^{Ru} R_{c,t}^{Ru} + C_{\mathrm{c}}^{Rd} R_{c,t}^{Rd}\right) \tag{13}$$

$$C_s^{RT,sys} = \sum_{t=1}^{N_T}\sum_{c=1}^{N_C}\left(\tilde{C}_c^{Ru}\tilde{R}_{c,t,s}^{Ru} + \tilde{C}_c^{Rd}\tilde{R}_{c,t,s}^{Rd}\right) + \theta^{VoLL}\sum_{t=1}^{N_T}\sum_{n=1}^{N_N}\tilde{L}_{n,t,s}^{Cur} \tag{14}$$

$$SU_{c,t} - SD_{c,t} = \left(o_{c,t} - o_{c,t-1}\right)\overline{C}_{c,t} \tag{15}$$

2) Constraints Involving First-stage Variables

The first-stage constraints are formulated with day-ahead point forecasting of all controllable components.

$$\underline{C}_{c,t} \le P_{c,t}^{\mathrm{c}} \le \overline{C}_{c,t} \quad \forall t, \forall g \tag{16}$$

$$\underline{SC}_{c,t} \le \sum_{t'=1}^{t} P_{g,t'}^{\mathrm{c}} \le \overline{SC}_{c,t} \quad \forall t, \forall g \tag{17}$$

$$\underline{DC}_{c,t} \le P_{c,t}^{\mathrm{c}} - P_{c,t-1}^{\mathrm{c}} \le \overline{DC}_{c,t} \quad \forall t, \forall g \tag{18}$$

$$\sum_{c=1}^{N_C} P_{c,t}^{c} = \sum_{n=1}^{N_N}\left(L_{n,t}^{fore} - L_{n,t}^{Cur}\right) \quad \forall t \tag{19}$$

$$-\overline{F}_l^L \le \sum_{n=1}\sum_{c\in\Omega_n} G_n^l P_{c,t}^{c} - \sum_{n=1}^{N_N} G_n^l\left(L_{n,t}^{fore} - L_{n,t}^{Cur}\right) \le \overline{F}_l^L \quad \forall t, \forall l \tag{20}$$

$$\sum_{c=1}^{N_C} R_{c,t}^{Ru} \ge R^{Ru,sys} \quad \forall t \tag{21}$$

$$\sum_{c=1}^{N_C} R_{c,t}^{Rd} \ge R^{Rd,sys} \quad \forall t \tag{22}$$

Among the above equations, (16)-(18) represent the power, energy and ramping constraints of each energy resource, respectively. Equation (19) represents the power balance constraint. Equation (20) represents the power flow constraints of all transmission lines. Equations (21) and (22) represent the constraints of up and down reserves.

3) Constraints Involving Second-Stage Variables

The second-stage constraints are formulated with real-time realization of each uncontrollable component together with the controllable component.

$$\underline{C}_{c,t} \le \tilde{P}_{c,t,s} \le \overline{C}_{c,t} + \tilde{P}_{c,t,s}^{\mathrm{u}} \quad \forall t, \forall c, \forall s \tag{23}$$

$$\underline{SC}_{c,t} \le \sum_{t'=1}^{t} \tilde{P}_{c,t',s} \le \overline{SC}_{c,t} \quad \forall t, \forall c, \forall s \tag{24}$$

$$\underline{DC}_{c,t} \le \tilde{P}_{c,t,s} - \tilde{P}_{c,t-1,s} \le \overline{DC}_{c,t} \quad \forall t, \forall c, \forall s \tag{25}$$

$$\sum_{c=1}^{N_C} \tilde{P}_{c,t,s} = \sum_{n=1}^{N_N}\left(L_{n,t}^{fore} - \tilde{L}_{n,t,s}^{Cur}\right) \quad \forall t, \forall s \tag{26}$$

$$-\overline{F}_l^L \le \sum_{n=1}^{N_N}\sum_{c\in\Omega_n} G_n^l \tilde{P}_{c,t,s} - \sum_{n=1}^{N_N} G_n^l\left(L_{n,t}^{fore} - \tilde{L}_{n,t,s}^{Cur}\right) \le \overline{F}_l^L \quad \forall t, \forall l, \forall s \tag{27}$$

In the above equations, (23)-(25) represent the power, energy, and ramping constraints of all energy resources, resepectively. Equation (26) represents the power balance constraint, and (27) represents the power flow constraints of each transmission line.

4) Linking Constraints Involving First- and Second-stage Variables

The first and second stages are linked together by the scheduled and deployed reserves.

$$\tilde{P}_{c,t,s} = P_{c,t}^{c} + \tilde{P}_{c,t,s}^{\mathrm{u}} - \tilde{R}_{c,t,s}^{Rd} + \tilde{R}_{c,t,s}^{Ru} \tag{28}$$

$$0 \le \tilde{R}_{c,t,s}^{Ru} \le R_{c,t}^{Ru} \tag{29}$$

$$0 \le \tilde{R}_{c,t,s}^{Rd} \le R_{c,t}^{Rd} + \max\left\{0, \tilde{P}_{c,t,s}^{\mathrm{u}}\right\} \tag{30}$$

Equation (28) demonstrates the relationship between day-ahead scheduled power and the deployed reserves. Equation (29) limits the deployed up reserves to be within the scheduled up reserves. Equation (30) limits the deployed down reserves to be within the scheduled down reserves. Note that (29) and (30) are asymmetrical because the upper bound of renewable energy is uncertain (due to the forecasting error), while the lower bound is certain (always equals to zero).

Since (30) is not a linear constraint, by introducing a slack variable $R_{c,t,s}^{slack}$ and adding a penalty term into the objective function, the constraint can be transformed into the linear constraint shown in (31)-(33).

$$0 \le \tilde{R}_{c,t,s}^{Rd} \le R_{c,t}^{Rd} + R_{c,t,s}^{slack} \tag{31}$$

$$R_{c,t,s}^{slack} \ge 0 \tag{32}$$

$$R_{c,t,s}^{slack} \ge \tilde{P}_{c,t,s}^{\mathrm{u}} \tag{33}$$

C. Aggregation of Cost Functions

As the marginal cost of renewables is nearly zero, the total energy cost of the system mainly depends on the energy cost of the thermal units and gas turbines. The energy cost of a thermal unit or a gas turbine can be expressed as a piecewise-linear function. The dispatch of thermal units depends on the incremental cost, i.e., the slope of the cost function. The lower the incremental cost is, the earlier the unit is scheduled. Hence, we can sort the piecewise curves of cost functions by their slopes and then recombine them end-to-end to obtain the aggregate cost function. An illustrative example of cost aggregation of three thermal units is shown in Fig. 3. The number above each line is the order of the slopes. It is clear that all objectives and constraints are linear; therefore, the model is a linear programming problem that can be efficiently solved by a linear programming solver.

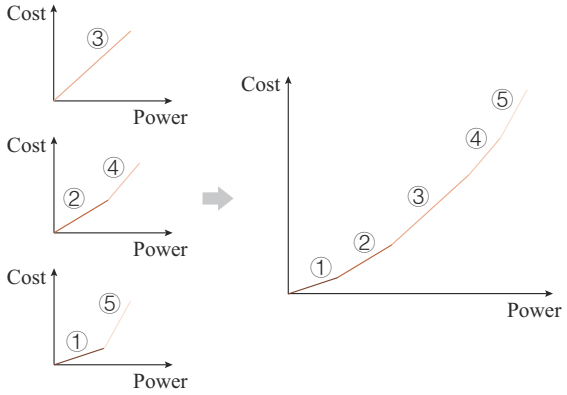

Fig. 3. Illustrative example of cost aggregation of three thermal units.

D. Discussions on Benefits of CUD-model-based SUC Model

It should be noted that the main benefit of aggregation is not to reduce the size of the SUC problem to increase the calculation speed. Instead, the main contribution of this paper is to propose a possible solution for incorporating massive distributed resources in the unit commitment problem.

Since it is unlikely for independent system operators (ISOs) to acquire the exact model of all the distributed resources due to the lack of information or privacy protection, the "detailed SUC model" that considers all the detailed parameters of distributed resources does not exist in actual practice. The ISO cannot formulate and solve the global "detailed SUC model" to reach a global optimal. We try to propose a model that can help ISO to dispatch the massive distributed resources without knowing the detailed model of these resources and to reach nearly optimal. We use the "detailed SUC model" as a metric in the next sections to demonstrate the effectiveness of the proposed aggregate model, not to improve the efficiency of the "detailed SUC model".

The potential of the proposed model could be foreseen under both market and non-market environments. In the electricity market, the proposed model is able to help the aggregators of distributed resources and microgrids to participate in the market as a virtual power plant, by aggregating the model of each resource together as an equivalent generator that has both flexibility and uncertainty. Under the non-market environment, the proposed model is useful for dispatching the generator companies that own distribution-level resources with both flexibility and uncertainty.

VI. Illustrative Example

A. Data Description

To test the capability of modeling both controllability and uncontrollability for the proposed model, an illustrative example is carried out on a three-bus system. The system data are extracted from [1]. Two wind farms and two thermal units (50 MW) are connected to buses 1 and 2, respectively. The proposed aggregation method is conducted on each bus of two wind farms and thermal units, which could be considered as the simplest aggregation demo. The rank correlation of wind farms at the same bus is 0.9, while the rank correlation of wind farms at bus 1 and bus 2 is 0.71. The load is located at bus 3, with an hourly load of 70, 120, 150, and 110 MW, respectively. The load is assumed to be a constant, i.e., the load uncertainty is ignored in the case study. The model is implemented in MATLAB and solved by CPLEX.

B. Results

This case is tested in two scenarios, i. e., the low-wind-power-penetration scenario and high-wind-power-penetration scenario. The capacity of each wind farm is set to be 15 MW and 75 MW, respectively. Figure 4 shows the scheduled and dispatched up and down reserves of the three-bus system in these two scenarios. Four color blocks represent the scheduled up and down reserves provided by thermal units and wind power.

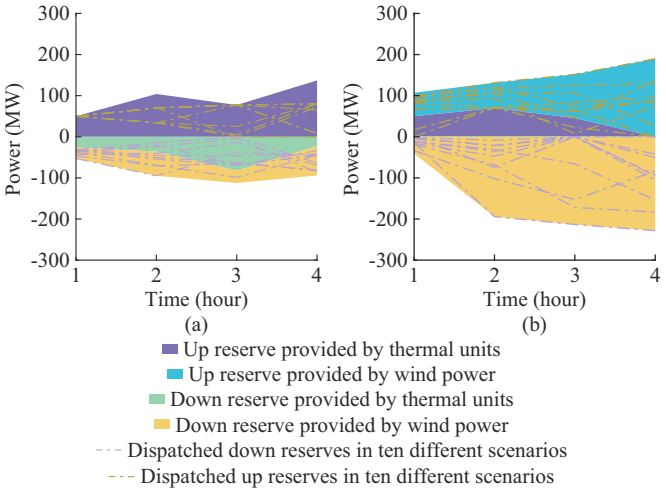

Fig. 4. Scheduled and dispatched up and down reserves of three-bus system. (a) Low-wind-power-penetration scenario. (b) High-wind-power-penetration scenario.

The results of the illustrative example show that the aggregation model facilitates the wind power to provide reserves like the thermal units, demonstrating that the decomposed modeling of controllability and uncontrollability is able to accurately describe the characteristics of energy resources with

different controllabilities so that their flexibility can be fully explored. It lays a foundation for further illustrating the effectiveness of exploring the flexibility of massive distributed energy resources using the aggregate model.

VII. Case Study: Qinghai Provincial Power Grid of China

A. Data Description

We apply the proposed method in Qinghai provincial power grid of China, a real power system in west China, to test the aggregation accuracy of the proposed model.

The daily load profile is extracted from the practical operation of Qinghai provincial power grid of China in 2018 with a maximum load of 8000 MW. The modified generation mix set of Qinghai provincial power grid of China is shown in Fig. 5. The total generation capacity is 27980 MW, including 15700 MW thermal and hydro, 2470 MW wind power, 9610 MW PV and 200 MW (400 MWh) energy storage. The capacity of variable renewable energy is 1.5 times the maximum load which requires great flexibility in daily operation.

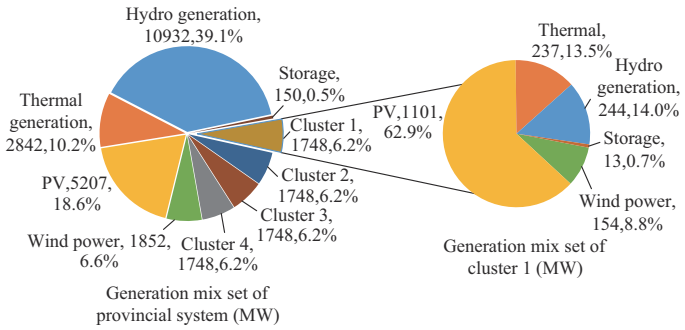

Fig. 5. Generation mix set of Qinghai provincial power grid of China.

To avoid wind power and PV curtailment, more renewable energy projects are co-installed with storage, hydro or thermal power generators such as Luneng Haixi 700 MW Wind, Solar, Heat and Storage Complementary Project [21]. The coordinated operation of small wind farms, PVs and other types of energy resources complicates the centralized dispatch of these resources. Hence, the proposed aggregation model could be used to efficiently dispatch these resources. To test the effectiveness of our model, we assume that 75% of the total capacity is scheduled as large-scale centralized generation, while the rest is made up of small distributed energy resources which belong to four aggregators. Each aggregator owns 100 units, including 20 wind, 40 PV, 20 thermal, 10 hydro, 10 storage, the numbers of each type of units are listed in Table I. The proposed methodology is conducted on the distributed energy resources to aggregate these resources into four clusters, named clusters 1-4. It should be noted that the settings of aggregators and the generation mix set in each aggregator are not practical data from Qinghai, since currently, there is not enough such complementary project. The purpose of such a setting is to test the effectiveness of our method on a real power system when there are massive distributed units that need to be aggregated.

TABLE I
Generation Mix Set of an Aggregator

Type	Number of units	Total capacity (MW)	Percentage (%)
Wind	20	154	8.8
PV	40	1101	62.9
Thermal	20	237	13.5
Hydro	10	244	14.0
Storage	10	13	0.7
Total	100	1749	100.0

B. Metrics of Comparison

In order to quantify the aggregation accuracy of the aggregate model to the detailed model, two metrics are evaluated. The results of the detailed model are indicated with the hat "^".

1) Operation Cost

The operation cost is the objective function value for optimization. The percentage difference is computed as:

$$\Delta^{Cost}=\frac{\left|C_{sys}-\hat{C}_{sys}\right|}{\hat{C}_{sys}}\times 100\% \tag{34}$$

2) Output Average Deviation

The percentage difference of the average deviation of scheduled output for each cluster is computed as:

$$\Delta^{Output}=\frac{\sum_{\forall c,\forall t}\left|P_{c,t}-\hat{P}_{c,t}\right|}{\sum_{\forall c,\forall t}\bar{P}_{c}}\times 100\% \tag{35}$$

C. Results

Table II shows a comparison of the detailed model and the aggregate model. The results illustrate that the aggregate model achieves a good aggregation performance on both operation cost and unit output in the real system.

TABLE II
Comparison Between Detailed Model and Aggregate Model on Qinghai Provincial Power Grid of China

Model	Operation cost (¥10^7)	Cost deviation (%)	Output average deviation (%)
Detailed model	2.9519		
Aggregate model	2.9567	0.16	1.50

The comparison of the total output of cluster 1 is shown in Fig. 6. The blue lines represent the output of the detailed model, while the red ones correspond to that of the aggregate model. The solid, dashed, and dash-dotted lines represent the day-ahead output, the real-time output in a low-renewable scenario, and the real-time output in a high-renewable scenario, respectively. It can be observed from Fig. 6 that the red lines are close to the blue lines, suggesting that

the proposed aggregate model is a good approximation of the detailed model in a real system.

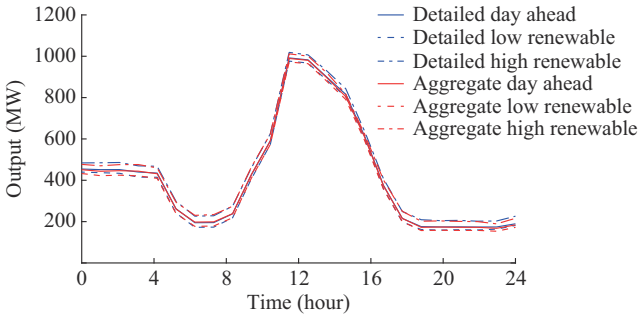

Fig. 6. Comparison of output between detailed and aggregate models on Qinghai provincial power grid of China.

VIII. Conclusion

To model and aggregate controllable and uncontrollable energy resources in power system operation, this paper proposes a CUD model for various energy resources. In this model, all types of energy resources are modeled by controllable and uncontrollable components. Such a unified decomposed modeling framework enables the aggregation of energy sources with different controllabilities. A two-stage SUC model using the proposed model is established. Case studies of a modified three-bus system and real Qinghai provincial power grid of China demonstrate that the proposed model is able to fully capture the uncertainty of energy resources while utilizing their flexibility.

References

[1] J. M. Morales, A. J. Conejo, and J. Perez-Ruiz, "Economic valuation of reserves in power systems with high penetration of wind power," *IEEE Transactions on Power Systems*, vol. 24, no. 2, pp. 900-910, May 2009.

[2] C. Zhao and Y. Guan, "Data-driven stochastic unit commitment for integrating wind generation," *IEEE Transactions on Power Systems*, vol. 31, no. 4, pp. 2587-2596, Jul. 2016.

[3] E. Du, N. Zhang, C. Kang *et al*., "Scenario map-based stochastic unit commitment," *IEEE Transactions on Power Systems*, vol. 33, no. 5, pp. 4694-4705, Sept. 2018.

[4] Y. Dvorkin, M. A. Ortega-Vazquez, and D. S. Kirschen, "Wind generation as a reserve provider," *IET Generation, Transmission & Distribution*, vol. 9, no. 8, pp. 779-787, May 2015.

[5] Y. Yang, M. Bao, Y. Ding *et al*., "Impact of down spinning reserve on operation reliability of power systems," *Journal of Modern Power Systems and Clean Energy*, vol. 8, no. 4, pp. 709-718, Jul. 2020.

[6] T. P. Teixeira and C. L. T. Borges, "Operation strategies for coordinating battery energy storage with wind power generation and their effects on system reliability," *Journal of Modern Power Systems and Clean Energy*, vol. 9, no. 1, pp. 190-198, Jan. 2021.

[7] M. Zhang, X. Ai, J. Fang *et al*., "A systematic approach for the joint dispatch of energy and reserve incorporating demand response," *Applied Energy*, vol. 230, pp. 1279-1291, Nov. 2018.

[8] Y. Jiang, J. Xu, Y. Sun *et al*., "Day-ahead stochastic economic dispatch of wind integrated power system considering demand response of residential hybrid energy system," *Applied Energy*, vol. 190, pp. 1126-1137, Mar. 2017.

[9] C. Vivekananthan, Y. Mishra, G. Ledwich *et al*., "Demand response for residential appliances via customer reward scheme," *IEEE Transactions on Smart Grid*, vol. 5, no. 2, pp. 809-820, Mar. 2014.

[10] M. Shafie-khah, E. Heydarian-Forushani, G. J. Osorio *et al*., "Optimal behavior of electric vehicle parking lots as demand response aggregation agents," *IEEE Transactions on Smart Grid*, vol. 7, no. 6, pp. 2654-2665, Nov. 2016.

[11] N. G. Paterakis, O. Erdinc, I. N. Pappi *et al*., "Coordinated operation of a neighborhood of smart households comprising electric vehicles, energy storage and distributed generation," *IEEE Transactions on Smart Grid*, vol. 7, no. 6, pp. 2736-2747, Nov. 2016.

[12] T. Zhang, S. Chen, H. Gooi *et al*., "A hierarchical EMS for aggregated BESSs in energy and performance-based regulation markets," *IEEE Transactions on Power Systems*, vol. 32, no. 3, pp. 1751-1760, May 2017.

[13] J. Liu, N. Zhang, C. Kang *et al*., "Cloud energy storage for residential and small commercial consumers: a business case study," *Applied Energy*, vol. 188, pp. 226-236, Feb. 2017.

[14] D. Pudjianto, C. Ramsay, and G. Strbac, "Virtual power plant and system integration of distributed energy resources," *IET Renewable Power Generation*, vol. 1, no. 1, pp. 10-16, Mar. 2007.

[15] E. G. Kardakos, C. K. Simoglou, and A. G. Bakirtzis, "Optimal offering strategy of a virtual power plant: a stochastic bi-level approach," *IEEE Transactions on Smart Grid*, vol. 7, no. 2, pp. 794-806, Mar. 2016.

[16] A. Baringo, L. Baringo, and J. M. Arroyo, "Day-ahead self scheduling of a virtual power plant in energy and reserve electricity markets under uncertainty," *IEEE Transactions on Power Systems*, vol. 34, no. 3, pp. 1881-1894, May 2019.

[17] E. Du, N. Zhang, C. Kang *et al*., "A high-efficiency networkconstrained clustered unit commitment model for power system planning studies," *IEEE Transactions on Power Systems*, vol. 34, no. 4, pp. 2498-2508, Jul. 2019.

[18] N. Zhang, C. Kang, Q. Xia *et al*., "Modeling conditional forecast error for wind power in generation scheduling," *IEEE Transactions on Power Systems*, vol. 29, no. 3, pp. 1316-1324, May 2014.

[19] N. Zhang, C. Kang, C. Singh *et al*., "Copula based dependent discrete convolution for power system uncertainty analysis," *IEEE Transactions on Power Systems*, vol. 31, no. 6, pp. 5204-5205, Nov. 2016.

[20] Y. Wang, N. Zhang, C. Kang *et al*., "An efficient approach to power system uncertainty analysis with high-dimensional dependencies," *IEEE Transactions on Power Systems*, vol. 33, no. 3, pp. 2984-2994, May 2018.

[21] China Solar Thermal Alliance. (2019, Aug.). Luneng Haixi multi-energy complementary integration optimization demonstration project. [Online]. Available: http://en.cnste.org/html/events/2019/0813/469.html

Hai Li received the B.S. degree from the Department of Electrical and Electronic Engineering of Huazhong University of Science and Technology, Wuhan, China, in 2017. He is now a Ph.D. candidate at Tsinghua University, Beijing, China. His research interests include energy storage, renewable energy, and power system planning and operation.

Ning Zhang received both the B.S. and Ph.D. degrees from the Electrical Engineering Department of Tsinghua University, Beijing, China, in 2007 and 2012, respectively. He is now an Associate Professor at the same university. His research interests include multiple energy system integration, renewable energy, and power system planning and operation.

Yue Fan received the Ph.D. degree from the Department of Electrical Engineering, Xi'an Jiaotong University, Xi'an, China, in 2000. He is now a Professorate Senior Engineer in State Grid Qinghai Electric Power Company, Xining, China. His main research interests include renewable energy penetration, power system stability and control.

Ling Dong received the M.S. degree from North China Electric Power University, Beijing, China, in 2007. She is now the General Manager of Qinghai Green Energy Data Co. Ltd of State Grid Qinghai Electric Power Company, Xining, China, and is currently persuing the Ph.D. degree in Tsinghua University, Beijing, China. Her research interests include power system dispatching and operation, renewable energy, and power system operation analysis.

Pengcheng Cai received the M.S. degree from Xinjiang University, Urumqi, China, in 2017. He is now a Senior Engineer of Power Dispatching Control Center of State Grid Xinjiang Electric Power Co., Ltd., Urumqi, China, and Director of Dispatching Control Department. His main research interests include new energy integration, new energy consumption, smart grid, etc.